α-Synuclein: Stable Compact and Extended Monomeric Structures and pH Dependence of Dimer Formation

Summer L. Bernstein, Dengfeng Liu, Thomas Wyttenbach, and Michael T. Bowers
Department of Chemistry and Biochemistry, University of California at Santa Barbara, Santa Barbara, CA, USA

Jennifer C. Lee, Harry B. Gray, and Jay R. Winkler
Beckman Institute, California Institute of Technology, Pasadena, CA, USA

The protein α-synuclein, implicated in Parkinson's disease, was studied by combining nano-electrospray ionization (N-ESI) mass spectrometry and ion mobility. It was found that both the charge-state distribution in the mass spectra and the average protein shape deduced from ion mobility data, depend on the pH of the spray solution. Negative-ion N-ESI of pH 7 solutions yielded a broad charge-state distribution from −6 to −16, centered at −11, and ion mobility data consistent with extended protein structures. Data obtained for pH 2.5 solutions, on the other hand, showed a narrow charge-state distribution from −6 to −11, centered at −8, and ion mobilities in agreement with compact α-synuclein structures. The data indicated that there are two distinct families of structures: one consisting of relatively compact proteins with eight or less negative charges and one consisting of relatively extended structures with nine or more charges. The average cross section of a-synuclein at pH 2.5 is 33% smaller than for the extended protein sprayed from pH 7 solution. Significant dimer formation was observed when sprayed from pH 7 solution but no dimers were observed from the low pH solution. A plausible mechanism for aggregate formation in solution is proposed. (J Am Soc Mass Spectrom 2004, 15, 1435–1443) © 2004 American Society for Mass Spectrometry

Parkinson's disease (PD) is the most common age-related neurodegenerative movement disorder caused by a loss of dopaminergic neurons in the substantia nigra region of the brain stem [1]. PD is among a family of amyloidogenic diseases including Alzheimer's, Huntington's, ALS, and Type II diabetes. The hallmark feature of PD is the presence in the cerebral cortex of intracellular inclusions, Lewy bodies and neurites [2, 3, 4]. Although PD is linked to the aggregation and fibril deposition of the protein α-synuclein (α-syn), the role of α-syn in the pathogenic process is unclear. Unfortunately, traditional techniques such as X-ray diffraction and NMR spectroscopy have been ineffective in elucidating the structure of the 140aa residue protein (Figure 1) because α-syn does not appear to have a well-defined native fold or detectable secondary structure [5, 6] in aqueous solution. Small-angle X-ray scattering studies show that α-syn has a radius of gyration (R_g ~ 40 Å) that is smaller than predicted for a fully extended random-coil conformation (52 Å) but larger than expected folded globular protein (15 Å) [7]. In the presence of acidic phospholipid vesicles, α-syn undergoes a conformational change, forming some α-helical structure observable by both CD and NMR spectroscopies [8]. Interestingly, in contrast to the monomeric protein, larger oligomeric α-syn intermediates cause membrane leakage, providing further support for the hypothesis that protofibrils rather than fibrils may be neurotoxic [9]. It also has been shown that, at higher protein concentrations (>100 μM), α-syn exhibits β-structure prior to fibril formation [10]. These findings that α-syn undergoes large environmentally induced conformational changes are of great interest; one or more of these species could disrupt cellular function through adverse membrane interaction, leading to PD.

N-ESI and ESI mass spectrometry has proven to be a useful technique for studying noncovalent interactions in select biopolymeric systems [11]. Studies by Robinson and co-workers using mass spectrometry on the self assembly of insulin aggregates involved in Type II

Published online September 11, 2004
Address reprint requests to Dr. Michael T. Bowers, Department of Chemistry and Biochemistry, University of California at Santa Barbara, Santa Barbara, CA, USA. E-mail: bowers@chem.ucsb.edu

1044-0305/04/$30.00
doi:10.1016/j.jasms.2004.08.003

Received April 14, 2004
Revised August 5, 2004
Accepted August 9, 2004

```
1           10          20          30          40
MDVFMKGLS   KAKEGVVAAA  EKTKQGVAEA  AGKTKEGVLY  VGSKTKEGVV
50          60          70          80          90
HGVATVAEKT  KEQVTNVGGA  VVTGVTAVAQ  KTVEGAGSIA  AATGFVKKDQ
100         110         120         130         140
LGKNEEGAPQ  EGILEDMPVD  PDNEAYEMPS  EEGYQDYEPE  A
```

Figure 1. Amino-acid sequence of human α-synuclein.

diabetes demonstrates that mass spectrometry can identify the solution states of oligomeric proteins [12]. Further, when mass spectrometry is coupled with ion mobility measurement [13, 14, 15] additional important information on molecular conformation can be obtained as shown in work by Bowers and co-workers [16, 17], Jarrold and co-workers [18], and Clemmer and co-workers [19, 20].

In this paper we employ mass spectrometry coupled to ion mobility measurements to probe the structure of monomeric α-syn and to give clues on the mechanism of aggregation of α-syn. In both instances we demonstrate the importance of initial solution conditions, especially solution pH, and that solution structures are essentially maintained in the solvent-free environment of the instruments used in the work reported here.

Experimental

Sample Preparation

The wild-type human α-syn expression plasmid (pRK172) [21] was provided by Dr. Ralf Langen (Keck School of Medicine, USC) and was chemically transformed into *E. coli* BL21(DE3)pLys-S cells (Stratagene Inc., La Jolla, CA). Recombinant α-syn was expressed and purified using minor modifications of published procedures [22]. Following boiling and acid precipitation steps, α-syn was chromatographed on a Q-Sepharose Fast Flow 16/10 column (Amersham Biosciences, Buckinghamshire, England) equilibrated with 20 mM Tris buffer (pH 8.0) and eluted with a linear gradient from 0 to 0.5 M NaCl. α-syn-containing fractions were pooled and further purified on a Mono-Q 10/10 column (Amersham Biosciences). Purity of the protein samples was assessed by SDS-PAGE on a Pharmacia Phastsystem (GMI Inc., Albertville, MN, USA). The molecular weight of recombinant protein was confirmed by ESI-MS (Caltech Protein/Peptide Microanalytical Laboratory, Pasadena, CA, USA). All solvents were purchased from Sigma (St. Louis, MO).

Samples for the N-ESI-MS/ion mobility experiment were prepared by dissolving lyophilized protein in water to make a 50 μM α-synuclein stock solution. Concentration of stock solution was determined using absorption spectroscopy with an extinction coefficient $\varepsilon(280\ nm) = 5120\ M_{-1}cm_{-1}$ [8]. pH 7 and pH 2.5 solutions in ammonium acetate buffer were prepared by dialysis of α-syn stock solution in 1L of 5mM ammonium acetate using Slide-a-lyzer Mini Dialysis Unit (3.5K MWCO, Pierce Biotechnology, Rockford, IL, USA) for 24 hours. pH was adjusted with HCl or NH_4OH to obtain the desired pH of the buffer solution.

Instrumental

Ion mobility coupled to mass spectrometry is a unique tool to explore the shape of polyatomic ions. The ion structure is obtained by measuring the collision cross sections in a high pressure drift tube filled with helium gas. Briefly, the instrument is composed of a nano-electrospray ionization (nano-ESI) source, an ion funnel, a drift cell, and quadrupole mass filter [23]. N-ESI gold metal coated borosilicate capillaries (0.1mm od/.78mm id), purchased from Proxeon, Germany, are filled with between 2 and 5uL of sample solutions. Ions are generated from solution in the nano-spray source which creates a continuous beam of ions that are injected into an ion funnel. The ion funnel is the interface to the vacuum system and can also be used as an ion storage device to convert the continuous ion beam into short ion pulses for cross section measurements [23]. Ions are then pulsed into the drift cell, where they are quickly thermalized by collisions with the helium buffer gas present at a pressure of 5 Torr. Due to the balance between the force imposed by the electric field (E) and the retarding force of friction, the ions obtain a constant drift velocity (v_D) which is proportional to E with the low field mobility K being the proportionality constant [24].

$$v_D = KE \tag{1}$$

The ions exiting the drift cell are analyzed in a quadrupole mass analyzer and detected as a function of time to obtain an arrival time distribution (ATD). Using kinetic theory it is possible to relate the ion mobility to the collision cross section σ and thus to the arrival time, t_A, at the detector:

$$\sigma = 1.3\left(\frac{q^2E^2T}{\mu k_B p^2 N^2 \ell^2}\right)^{1/2}(t_A - t_0) \tag{2}$$

where q is the ion charge, T the temperature in Kelvins, p the pressure in Torr, μ the reduced mass of the ion-He collision, k_B the Boltzmann constant, N the He number density at STP, the cell length and t_0 the time the ion spends after exiting the mobility cell before hitting the

detector. The ion mobility process allows us to separate ions of the same mass-to-charge (m/z) ratio that may have different conformations. Ions with compact conformations have a small cross section and large mobility, and the opposite is true for extended structures.

Molecular Modeling

Model structures were generated by molecular mechanics for comparison of their cross sections with experiment. An extended all-α-helical conformer and a compact globular conformer were assembled using the standard AMBER [25] amino acid residues with all basic sites (amino groups) protonated and all acidic sites (carboxylic acids) deprotonated. All calculations were carried out on structures in the absence of solvent. The α-helical conformation was obtained by setting all ϕ and Ψ angles to -57° and -47°, respectively (see for example, [26]). The globular structure was the most compact structure located from a set of 100 candidate structures. The candidate globular structures are the result of the following sampling procedure. Geometries were sampled every 30 ps during a 3 ns dynamics run at 800 K and each geometry was rapidly cooled to 0 K using a linear temperature profile with a slope of 80 K/ps and subsequent energy minimization. As this type of temperature profile is not expected to allow sufficient equilibration the resulting candidate structures are most likely not properly annealed. However, the most compact of these structures appear to be tightly packed and near spherical and provide a good lower limit for both the radius of gyration and the cross section for this size protein. Cross sections of model structures were obtained using the exact hard sphere scattering procedure [27].

Results and Discussion

Mass spectra in both positive and negative ion mode were obtained for α-syn with various initial pH solutions. However, since α-syn is a negatively charged protein in solution (excess charge of -9) at pH 7 the negative ion spectra will be discussed here. The negative ion mass spectra of α-syn for pH 2.5 and pH 7 solutions in 5mM ammonium acetate are shown in Figure 2. The mass spectrum of the protein from pH 2.5 solutions (Figure 2a) shows a narrow charge state distribution from -6 to -11 with a sharply peaked maximum intensity at -8. Protein sprayed from neutral pH solution (Figure 2b) exhibits a spectrum with a broader charge state distribution that includes additional charge states -12 to -16 with a new maximum intensity at -11. Interestingly, α-syn dimers also are observed with charge states -17 to -21 (Figure 2b). The solutions do not form a stable spray under basic conditions (in either positive or negative ion mode) so no mass spectra were obtained from solutions with pH greater than 7.

It has long been accepted that initial solution pH affects charge state distributions of proteins observed by ESI-MS, a phenomenon that has been attributed to changes in the solution-phase conformations [28]. For a typical protein, a charge state distribution centered at low charge states indicates the presence of folded conformations (fewer sites exposed for deprotonation during the electrospray process), whereas a distribution of higher charge states indicates the protein exists in more extended conformations [28, 29]. Hence, the α-syn mass spectrum from a pH 2.5 solution (Figure 2a) suggests the presence of compact conformations under acidic solution conditions, whereas the spectrum from pH 7 solutions (Figure 2b) suggests more open conformations. Most proteins unfold at low pH but α-syn has a very acidic C-terminal region which upon protonation can lead to protein collapse and compact structures. α-syn is considered to be one of the 90 or more proteins known to be intrinsically disordered at neutral pH [30] and our conclusions based on mass spectrometry are in qualitative agreement with results obtained using far-UV circular dichroism, fluorescence, FTIR, NMR, and small angle x-ray scattering (SAXS) methods [8, 32]. These researchers conclude that α-syn is "natively unfolded" at neutral pH because of its low intrinsic hydrophobicity and high net negative charge. Thus lowering the pH decreases the net charge of α-syn which Uversky et al. [31] suggest results in the partial folding of the molecule. The charge reduction as pH is lowered is evident in the mass spectra of Figure 2.

Figure 3 shows the ATDs for the -7, -8 and -9 charge states of α-syn obtained from pH 2.5 solutions at several injection energies. At low injection voltages the ions are gently pulsed into the mobility cell and only need a few "cooling" collisions to reach thermal equilibrium with the buffer gas. At high injection voltage the larger collision energy leads to internal excitation of the ions before cooling and equilibration occur. This transient internal excitation can lead to annealing, i.e., partial or complete isomerization to the most stable conformers or, if they are present, dissociation of dimers and higher aggregates [32]. Understanding this process allows interpretation of the ATDs in Figure 3.

At low injection voltage (20 V) the ATD for the -7 charge state of α-syn (Figure 3a) has a narrow distribution at relatively short arrival time. The narrowness of the ATD is consistent with a single family of conformers and the relatively low cross section of 1425 $Å^2$ indicates these conformers are compact. At an intermediate injection voltage of 40 V the ATD becomes broader, displaying multiple features that are interpreted as less compact isoforms of the initial structure observed at the lowest injection energy. By 100 V a narrow distribution at longer time is observed, indicating the compact "solution structures" obtained at low injection energies have been annealed to a family of more extended structures with a cross section of 1762 $Å^2$. These data provide compelling evidence that when compact solution structures of α-syn are sprayed, substantial internal

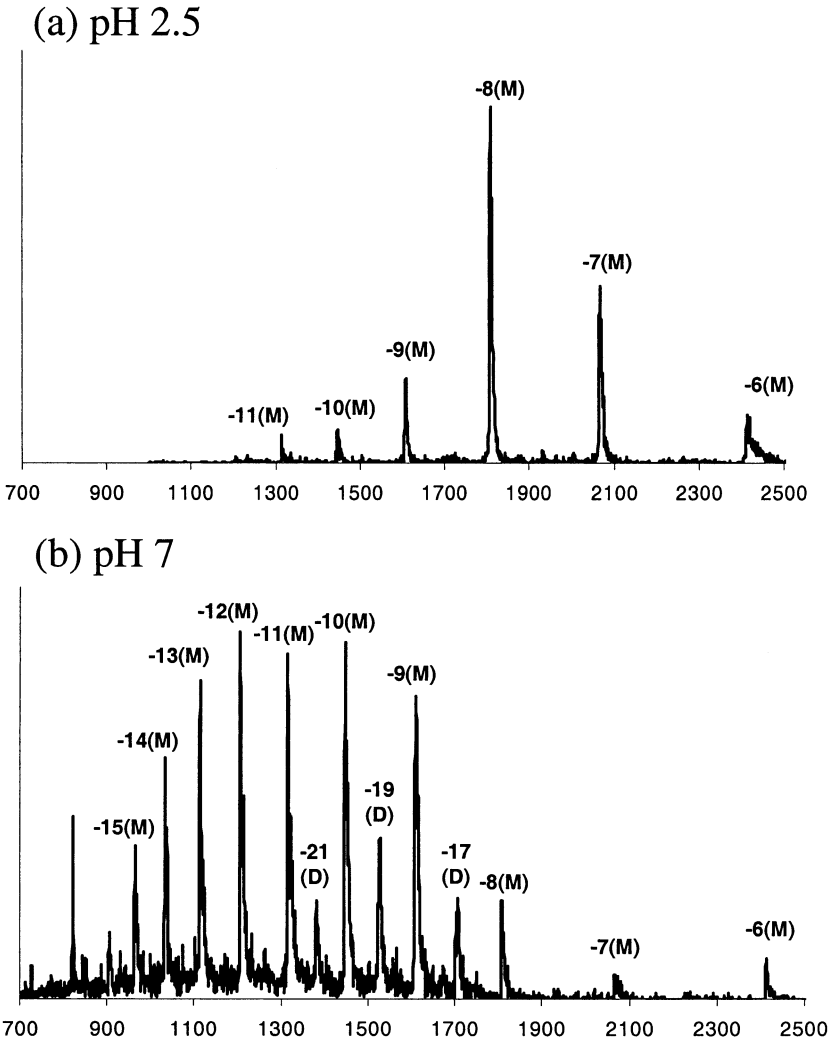

Figure 2. Nano-ES deprotonated mass spectrum of α-synuclein 5 mM ammonium acetate buffer at pH 2.5. The dominant charge state is −8 monomer. There is no dimer charge state distribution present at pH 2.5 **(b)** Nano-ES deprotonated mass spectrum of α-synuclein in 5 mM ammonium acetate buffer at pH 7.0. The charge states labeled with M and D represent monomeric and dimeric α-synuclein. The dominant charge state distribution corresponds to monomers and a secondary charge state distribution to dimers. Notice that the dimers are only labeled for the odd charge states since the even charge states for the dimers have the same m/z values as the corresponding monomers.

excitation is required to isomerize them to more stable solvent free isoforms.

The -8 ion (Figure 3b) reacts much like the -7 charge state as injection energy is varied. However, the -9 charge state has only one extended family of structures regardless of injection energy (Figure 3c), indicating an extended "solution structure" is being sprayed. Similar results are found for charge states above −9.

Cross sections obtained from the ATDs of the various charge states are plotted in Figure 4. Clearly, two distinct types of α-syn structures are observed; a family of compact structures prominent in charge states −6 through −8 (solid circles in Figure 4) and a second family of extended structures carrying 9 and more negative charges (open circles in Figure 4). The transition from one population to the other occurs between charge state −8 and −9 with an increase in cross section of over 50% (~800 Å^2). Cross sections of extended conformations increase with increasing charge state indicating that structures continue to elongate as more charges are added, presumably due to Coulombic repulsion between the negative charges. Also shown as dashed lines in Figure 4 are the cross sections calculated for the two model structures described in the "Molecular Modeling" section; the all-helical conformation and the compact globular structure. Neither of these two structures is expected to be a realistic model of the actual protein but is intended to be a "yardstick" for comparison with the experimental data; the helix an extreme extended structure and the globule a compact structure. It is evident that the cross sections of charge states −6 through −8 are in good agreement with the theoretical cross section of the compact globular structure, confirming these charge states are (partially) col-

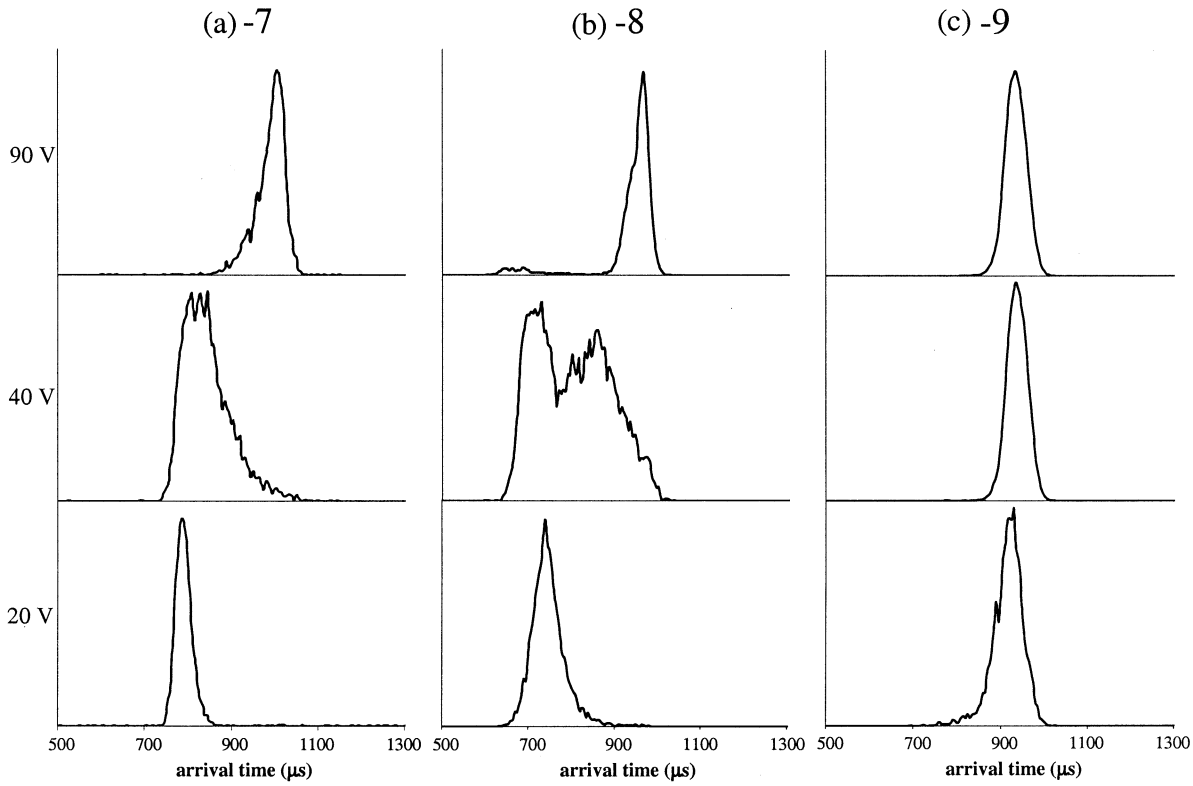

Figure 3. **(a)** Arrival Time Distributions (ATDs) for α-syn -7 charge state at 20V, 40, and 100V Injection energy. **(b)** ATD injection dependence for α-syn −8 charge state. **(c)** ATD injection dependence for α-syn −9 charge state.

lapsed forms of the protein. The experimental cross sections of the −9 and higher charge states (open circles in Figure 4) are much larger than the globular theoretical structure, but not as extended as the all-helical structure, consistent with substantially unfolded structures.

The question arises as to how the structures of species observed in solvent-free environments correlate with those present in the solution they are sprayed from. While this point has been addressed above, further discussion is useful. Clearly, solution properties are reflected in the charge state distributions shown in Figure 2. Changing a solution property, pH, dramatically changes the mass spectrum even though the spray conditions were essentially unchanged. When spraying from pH 7 solutions, the charge state distribution is centered about charge state −11. As expected, lowering the pH reduces the negative charge on α-syn and narrows the distribution, centering it at about -8.

The ion mobility results indicate a dramatic change in structure occurs with pH as well. From the cross section data in Figure 4 and the mass spectra in Figure 2 we can estimate how the average "shape" of α-syn varies with solution pH: at pH 7 relatively open structures are obtained (σ_{avg} = 2530 Å^2), whereas at pH 2.5 more globular, compact structures occur (σ_{avg} = 1690 Å^2). These results nicely correlate with the findings of Fink and coworkers [31] where they found the radius of gyration decreased by about 25% going from pH 7 to pH 3 as measured by small angle X-ray scattering (see Figure 4). Our measured average cross section decreases 33% over a slightly larger pH range. While radius of gyration and cross section do not map one to one, the agreement is apparent.

There is compelling evidence for very large systems (in the 1 megadalton range) that the solvent-free ions formed by electrospray do in fact retain solution-phase structures [33]. Conversely, for small peptides and synthetic polymers it is clear that solution structures are lost and the ions rearrange to preferred solvent-free configurations [16, 34]. In between, the situation is not so clear. For the amyloid β-peptide, Aβ42, implicated in Alzheimer's disease, there is evidence that the solution structure is essentially retained when the water solvent evaporates. The peptide does "shrink" somewhat when dehydrated as intramolecular interactions replace peptide–H_2O interactions but the backbone integrity is retained [35].

For relatively small nucleotide complexes it also appears that solution structures are retained when they are sprayed. For example, $(dCG)_7$ duplexes form helices in solution and a helix motif is retained following dehydration according to ion mobility results [36, 37]. Even systems as small as $(guanosine)_4Na^+$, which forms a quadruplex in solution, has its structure maintained when sprayed and the water evaporates, even though

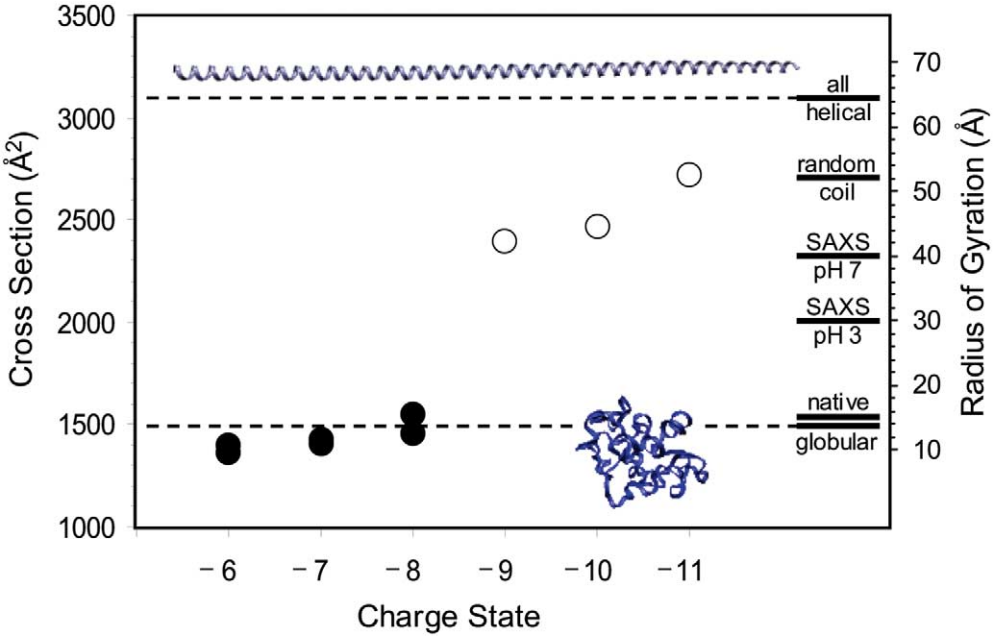

Figure 4. Plot of cross section versus charge for the dominant peaks in the ATDs measured for samples at pH 7. Filled circles represent compact structures and open circles represent extended structures. Dashed lines represent cross sections calculated for two model structures, an all-helical conformation and a compact globular structure. Neither one of these two structures are expected to be realistic models of the actual protein, they are simply included as a "yard stick" to gauge the experimental data. Plotted on the right hand side are radii of gyration: "globular" and "all-helical" are calculated values for the corresponding theoretical structures; "SAXS pH 3" and "SAXS pH 7" are experimental data (small angle scattering studies) from [32]; "random coil" and "globular" are estimated values [32].

modeling suggests a globular structure is lower in energy [37, 38].

For very large systems, especially aggregates like the chaperonin GroEL [39], it is reasonable that dehydration does not affect structure. For smaller systems the key issues are whether solvent-free and solvated structures are intrinsically the same or different and if different what are the rearrangement barriers. It is useful to view the process as follows:

$$\begin{aligned}
&(P)^{-z}(H_2O)_x \text{ Solution Structure}\\
&\quad\downarrow \text{Spray}\\
&(P)^{-z}(H_2O)_x \text{Droplet}\\
&\quad\downarrow \text{Evaporation}\\
&(P)^{-z}(H_2O)_{x-1} + H_2O\\
&\quad\cdots\\
&\quad\downarrow \text{Evaporation}\\
&(P)^{-z} + xH_2O\\
&\quad\downarrow \text{Ionmobility}\\
&(P)^{-z}\text{Solvent-free structure}
\end{aligned} \tag{3}$$

where $(P)^{-z}$ is a protein with z negative charges. While this scheme is not meant to accurately reflect the electrospray process, it does reasonably portray the journey of a given α-syn protein as it makes its way from solution to the instrument detector. The charged ion is gradually desolvated requiring some intramolecular adjustments to better self-solvate the charge sites. This process leads to a somewhat more compact molecule than one found in solution but does not necessarily facilitate massive rearrangement to the most stable solvent-free family of structures. The results presented here suggest solution like structures are sampled in ion mobility experiments on α-syn.

The effect of a single charge on the structure of α-syn can be very dramatic. It is apparent from the cross section data in Figure 4 that the protein goes from a predominantly collapsed/globular family of structures for the -8 (and lower) to a predominantly extended family of structures state at charge state -9 (and higher). While it is not unusual for proteins to undergo conformational change with charge state [18], usually a major "unfolding" transition occurs over 3 or 4 charge states and the cross-sectional change per charge state is far less than the 50% change observed here. A second difference is the conformational change results for α-syn are for a negatively charge protein where most other results in the literature are for positively charged molecules.

Our data suggests the protein charge state may be an important factor in initiating amyloid formation of α-syn. One way to reduce charge is to ligate a protein with metal ions. A study of seven natively unfolded

proteins suggests metal ion ligation can induce and accelerate aggregation [7]. If indeed folding is required for aggregation, as appears necessary from measurements of the width of amyloid fibrils formed from α-syn [6, 10], the binding of α-syn to one or more metal ions may induce conformational change and thus have implications for the onset PD. These systems are currently under study and the results will be published elsewhere.

The mass spectrum of α-syn from pH 7 solution (Figure 2b) has an interesting feature. Dimer peaks at −17 to −21 are observed with significant intensity. This observation is perhaps surprising since we have been discussing the fact that in solution low pH (low charge states) accelerates fibril formation. Yet, at low pH (Figure 2a) there is no sign of dimer formation. An analogous situation occurs in the Alzheimer's peptide Aβ42 wt, which is known to form amyloid fibrils rapidly while a mutant F19P does not appear to form them at all [40]. In the mass spectra, no dimer is observed for the Aβ42 wt, only a weak monomer signal. Evidence for fibril formation is clear, however, as our nanospray tips rapidly clog for the wt peptide [35]. On the other hand, significant dimer is observed in the mass spectra for the F19P mutant. However, no tip clogging occurs, the solutions spray beautifully and signal levels are an order of magnitude higher than for Aβ42 wt. Our explanation for these results is that dimer formation is in fact occurring for Aβ42 wt but before the dimer can be observed in the mass spectrum it rapidly moves on to higher aggregates [35]. The F19P mutant also forms dimers (and tetramers) but does not form higher-order aggregates and hence can be observed. The implication is the structures of the dimers are significantly different in the two species.

A parallel situation may be occurring in α-syn with two important differences. First, the species involved are the compact wt protein at low pH and an extended wt protein at pH 7. No mutants are involved. Second, and most important, the fibrillization rates for *both* the folded and the extended protein are slow since no tip clogging is observed regardless of the pH of the solution sprayed. A plausible mechanism that is consistent with our results and with the fact others observe accelerated fibrillization at low pH in α-syn is given below:

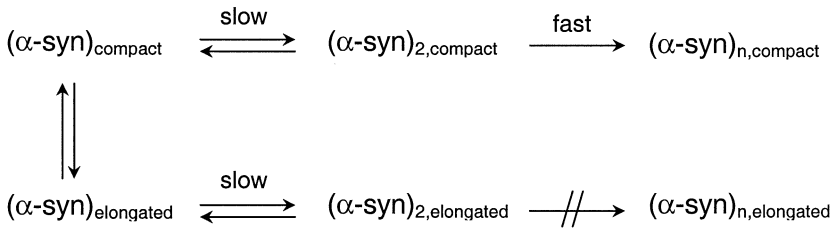

For compact α-syn monomer (i.e., low pH form) formation of the dimer is rate limiting. Once the dimer forms it rapidly aggregates further to form higher oligomers outside the *m/z* range of out experiment. Fibril formation must occur at substantially smaller rates than for Aβ42 wt, however, since tip clogging is not observed. The rate of dimerization of elongated α-syn also appears to be slow, as evidence by the fact monomer intensities are substantially greater than the dimer intensities (Figure 2b). The fact that we observe dimers at pH 7 at all suggests that further aggregation of the species is very slow on our experimental time scale. It also suggests that dimers formed from compact α-syn must have substantially different structures than those formed from elongated α-syn. Conformation of the mechanism awaits experiments designed to detect higher oligomers of α-syn and how their formation depends on solution pH.

Summary and Conclusions

1) ESI mass spectra obtained by spraying neutral pH solutions yield a broad charge state distribution peaking at charge state −11 suggestive of extended conformations in solution. N-ESI mass spectra of pH 2.5 solutions show a narrow charge state distribution with a maximum intensity at −8 suggestive of (partially) folded conformations in solution.
2) Ion mobility results demonstrate that low charge states occurring at low pH have small cross sections (~1500 Å^2) and are compact while high charge states occurring at physiological pH have larger cross sections (> 2400 Å^2) and are relatively unfolded. The transition from compact to elongated structures occurs from charge state −8 to −9 where a 50% increase in cross section is observed. Since the excess charge on α-syn is −9, (at pH 7), only small perturbations in solution properties are required to dramatically change the conformations of the protein (metal ions, pH, etc.).
3) The combined data of mass spectral charge distributions and charge-state dependent cross sections indicates the presence of compact structures (σ_{avg} = 1690 Å^2) when spraying low-pH solutions and extended structures (σ_{avg} = 2530 Å^2) when spraying neutral solutions (pH = 7). Our results are in agreement with solution studies by Fink and co-

workers who have found that α-syn is "natively unfolded" at neutral pH (radius of gyration ~40 Å) and partially collapsed at low pH (radius of gyration ~30 Å) [32].

4) Dimer was observed in the mass spectrum sprayed from pH 7 while not from those sprayed from pH 2.5 solutions. This is the first time a dimer has been reported for α-syn. The dimers formed at pH 7 are extended and do not appear to further aggregate. If dimers are formed in low pH solutions, they rapidly form higher order oligomers out of the *m/z* range of our experiment.
5) Our results suggest that solution structures of α-syn are essentially retained in the gas phase and that the combination of ion mobility and mass spectrometry is useful tool for studying structures that are difficult to obtain by conventional solution techniques.

Acknowledgements

This research was supported by a grant from the National Science Foundation, CHE-0140215 (MTB), Beckman Macular Research Center (HBG), Parkinson's Disease Foundation and National Parkinson Foundation (JRW), and the Beckman Foundation for a Beckman Senior Research Fellowship (JCL).

References

1. Dunnett, S. B.; Bjorklund, A. Prospects for new restorative and neuroprotective treatments in Parkinson's disease. *Nature Suppl.* **1999,** *399(6738),* A32–A39.
2. Baba, M.; Nakajo, S.; Tu, P. H.; Tomita, T.; Nakaya, K.; Lee, V. M. Y.; Trojanowski, J. Q.; Iwatsubo, T. Aggregation of Alpha-synuclein in Lewy bodies of sporadic Parkinson's disease and dementia with Lewy Bodies. *Am. J. Path.* **1998,** *152,* 879–884.
3. Spillantini, M. G.; Schmidt, M. L.; Lee, V. M. Y.; Trojanowski, J. Q.; Jakes, R.; Goedert, M. Alpha-synuclein in Lewy bodies. *Nature* **1997,** *388,* 839–840.
4. Selkoe, D. J. Translating cell biology into therapeutic advances in Alzheimer's disease. *Nature Suppl.* **1999,** *399,* A23–A31.
5. Bussell, R.; Eliezer, D. Residual structure and dynamics in Parkinson's disease-associated mutants of alpha-synuclein. *J. Biol. Chem.* **2001,** *276,* 45996–46003.
6. Serpell, L. C.; Berriman, J.; Jakes, R.; Goedert, M.; Crowther, R. A. Fiber diffraction of synthetic alpha-synuclein filaments shows amyloid-like cross-beta conformation. *Proc. Natl. Acad. Sci. USA* **2000,** *97,* 4897–4902.
7. Uversky, V. N.; Li, J.; Fink, A. L. Metal-triggered structural transformations, aggregation, and fibrillation of human alpha-synuclein—A possible molecular link between Parkinson's disease and heavy metal exposure. *J. Biol. Chem.* **2001,** *276,* 44284–44296.
8. Eliezer, D.; Kutluay, E.; Bussell, R.; Brown, G. Conformational properties of alpha-synuclein in its free and lipid-associated states. *J. Mol. Biol.* **2001,** *307,* 1061–1073.
9. Volles, M. J.; Lee, S. J.; Rochet, J. C.; Shtilerman, M. D.; Ding, T. T.; Kessler, J. C.; Lansbury, P. T. Vesicle permeabilization by protofibrillar alpha-synuclein: Implications for the pathogenesis and treatment of Parkinson's disease. *Biochemistry* **2001,** *40,* 7812–7819.
10. Conway, K. A.; Harper, J. D.; Lansbury, P. T. Accelerated in vitro fibril formation by a mutant alpha-synuclein linked to early-onset Parkinson disease. *Nature Med.* **1998,** *4,* 1318–1320.
11. (a) Benjamin, D. R.; Robinson, C. V.; Hendrick J. P.; Hartl, U.; Dobson, C. M. Mass Sepctrometry of Ribosomes and Ribosomal subunits. *Proc. Nat. Acad.* **1998,** *95,* 7391–7395; (b) Rostom, A. A.; Fucini, P.; Benjamin, D. R.; Juenemann, R.; Nierhaus, K. H.; Hartl, F. U.; Dobson, C. M.; Robinson, C. V. Detection and selective dissociation of intact Ribosomes in a mass spectrometer. *Proc. Natl. Acad. Sci.* **2000,** *97,* 5185–5190.
12. Nettleton, E. J.; Tito, P.; Sunde, M.; Bouchard, M.; Dobson, C. M.; Robinson, C. V. Characterization of the oligomeric states of insulin in self-assembly and amyloid fibril formation by mass spectrometry. *J. Biophys.* **2000,** *79,* 1053–1065.
13. von Helden, G; Hsu, M. T.; Kemper, P. R.; Bowers, M. T. Structures of carbon cluster ions from 3 to 60 atoms: Linears to rings to fullerenes. *J. Chem. Phys.* **1991,** *95,* 3835–3837.
14. Clemmer, D. E.; Jarrold, M. F. Ion Mobility measurements and their applications to clusters and biomolecules. *J. Mass Spectrom.* **1997,** *92,* 577.
15. Wyttenbach, T.; Bowers, M. T. Gas-Phase conformations: The Ion Mobility/Ion Chromatography method. *Top. Curr. Chem.* **2003,** *225,* 207–232.
16. Wyttenbach, T.; von Helden, G.; Bowers, M. T. Gas-Phase conformation of biological molecules: Bradykinin. *J. Am. Chem. Soc.* **1996,** *118,* 8355–8364.
17. (a) Gidden, J.; Wyttenbach, T.; Jackson, A. T.; Scrivens J. H.; Bowers, M. T. Gas-phase conformations of synthetic polymers: Poly(ethylene glycol), Poly(propylene glycol), and Poly(tetramethylene glycol). *J. Am. Chem. Soc.* **2000,** *122,* 4692–4699; (b) Gidden, J.; Bowers, M. T. Gas-phase conformations of deprotonated trinucleotides ($dGTT^-$, $dTGT^-$, and $dTTG^-$): The question of zwitterion formation. *J. Am. Soc. Mass Spectrom.* **2003,** *14,* 161–170.
18. (a) Clemmer, D. E.; Hudgins, R. R.; Jarrold, M. F. Naked protein conformation: Cytochrome c in the gas phase. *J. Am. Chem. Soc.* **1995,** *117,* p. 1014; (b) Shelimov, K. B.; Clemmer, D. E.; Hudgins, R. R.; Jarrold, M. F. Protein structure in vacuo: Gas-phase conformations of BPTI and Cytochrome c. *J. Am. Chem. Soc.* **1997,** *119,* 2240; (c) Hudgins, R. R.; Ratner, M. A.; Jarrold, M. F. Design of helices that are stable in vacuo. *J. Am. Chem. Soc.* **1998,** *120,* 12974; (d) Kohtani, M.; Kinnear, B. S.; Jarrold, M. F. Metal-ion enhanced helicity in the gas phase. *J. Am. Chem. Soc.* **2000,** *122,* 12377.
19. Li, J.; Taraszka, J. A.; Counterman, A. E.; Clemmer, D. E. Influence of solvent composition and capillary temperature on the conformations of electrosprayed ions: unfolding of compact ubiquitin conformers from pseudonative and denatured solutions. *Int. J. Mass Spectrom.* **1999,** *185,* 37.
20. Counterman, A. E.; Clemmer, D. E. Large Anhydrous Polyalanine ions: Evidence for extended helices and onset of a more compact state. *J. Am. Chem. Soc.* **2001,** *123,* 1490.
21. Jakes, R.; Spillantini, M. G.; Goedert, M. Identification of 2 distinct synucleins from human brain. *FEBS Lett.* **1994,** *345,* 27–32.
22. Der-Sarkissian, A.; Jao, C. C.; Chen, J.; Langen, R. Structural organization of alpha-synuclein fibrils studied by site-directed spin labeling. *J. Biol. Chem.* **2003,** 37530–37535.
23. Wyttenbach, T.; Kemper, P. R.; Bowers, M. T. Design of a New Electrospray Ion Mobility Mass Spectrometer. *Int. J. Mass Spectrom.* **2001,** *212,* 13–23.
24. Mason, E. A.; McDaniel, E. W. *Transport Properties of Ions in Gases.* Wiley, New York 1978.
25. Case, D. A.; Pearlman, D. A.; Caldwell, J. W.; Cheatham, T. E. III; Wang, J.; Ross, W. S.; Simmerling, C. L.; Darden, T. A.; Merz, K. M.; Stanton, R. V.; Cheng, A. L.; Vincent, J. J.; Crowley, M.; Tsui, V.; Radmer, R. J.; Duan, Y.; Pitera, J.; Massova, I.; Seibel, G. L.; Singh, U. C.; Weiner, P. K.; Kollman, P. A. *AMBER 7*; Unversity of California: San Francisco, 2002.

26. Mathews, C. K; van Holde, K. E. *Biochemistry.* Benjamin/Cummings, Redwood City, California; 1990.
27. Shvartsburg, A. A.; Jarrold, M. F. An Exact hard-spheres scattering model for the mobilities of polyatomic ions. *Chem Phys Let.* **1996,** *261,* 86–91.
28. Chowdhury, S. K.; Katta, V.; Chait, B. T. Probing conformational changes in proteins by mass spectromery. *J. Am. Chem. Soc.* **1990,** *112,* 9012–9013.
29. Jarrold, M. F. Peptides and proteins in the vapor phase. *Annu. Rev. Phys. Chem.* **2000,** *51,* 179–207.
30. Uversky, V. N.; Gillespie, J. R.; Fink, A. L. Why are "Natively unfolded" proteins unstructured under physiologic conditions? *Proteins: Struct, Funct, and Genetic.* **2000,** *41,* 415–427.
31. Uversky, V. N.; Li, J.; Fink, A. L. Evidence of partially folded intermediate in a-synuclein fibril formation. *J. Biol. Chem.* **2001,** *276,* 10737–10744.
32. von Helden, G.; Gotts, N. G.; Bowers, M. T. Experimental evidence for the formation of Fullerenes by collisional heating of carbon rings in the gas phase. *Nature* **1993,** *363,* 60–63.
33. Last, A. M.; Robinson, C. V. Protein folding and interactions revealed by Mass Spectrometry. *Curr. Opin. Chem. Biol.* **1999,** *3,* 564–570.
34. Wyttenbach, T.; von Helden, G.; Bowers, M. T. Conformations of alkali ion cationized Polyethers in the gas phase: Polyethylene Glycol and Bis[(benzo-15-crown-5)-15-ylmethyl Pimelate. *Int. J. Mass Spectrom. Ion Proc.* **1997,** *165,* 377; Gidden, J; Bushnell, J. E.; Bowers, M. T. Gas-Phase Conformations and Folding Energetics of Oligonucleotides: dTG^- and dGT^-. *J. Am. Chem. Soc.* **2001,** *123,* 5610–5611.
35. Bernstein, S. L.; Wyttenbach, T.; Baumketner, A.; Shea J.-E.; Bitan, G.; Teplow, D. T.; Bowers, M. T. Amyloid β-protein: Monomer structure and early aggregation states of Aβ42 and its Pro^{19} alloform. *J. Am. Chem. Soc.* (submitted).
36. Gidden, J.; Ferzoco, A.; Baker, E. S.; Bowers, M. T. Duplex formation and the onset of helicity in dCG oligonucleotides in a solvent-free environment. *J. Am. Chem. Soc.* (in press).
37. Gidden, J.; Baker, E. S.; Ferzoco, A.; Bowers, M. T. Structural motifs of DNA complexes in the gas phase. *Int. J. Mass Spectrom.* (in press).
38. Baker, E. S.; Bernstein, S. L.; Bowers, M. T. (mss in preparation).
39. Rostam, A. A.; Robinson, C. V. Detection of Intact GroEL chaperonin assembly by Mass Spectrometry. *J. Am. Soc.* **1999,** *121,* 4718–4719.
40. Bitan, G.; Kirkitadze, M. D.; Lomakin, A.; Vollers, S. S.; Benedek, G. B.; Teplow, D. B. Amyloid β-protein (Aβ) assembly: Aβ40 and Aβ oligomerization through distinct pathways. *Proc. Natl. Acad. Sci. USA* **2003,** *100(1),* 330–335.